Met.O.816
METEOROLOGICAL OFFICE

the meteorological magazine

OCTOBER 1969 No 1167 Vol 98
Her Majesty's Stationery Office

Recent Meteorological Office Publication

Tables of surface wind speed and direction over the United Kingdom

Table I presents average frequencies of wind speed and direction at 21 selected stations for the period 1950 to 1959. Table II contains means and maxima of the highest hourly wind speeds at 73 stations and Table III presents the means and maxima of the highest monthly gusts. Tables IV to IX give, for 43 anemograph stations, the average number of days in each month and the year on which gust speeds exceeded 33, 40, 50 and 60 knots and the average number of hours in each month and the year with gusts exceeding 33 and 47 knots. Table X consists of monthly and annual average percentage frequencies of hourly mean wind speeds and directions combined. Tables XI and XII give, for hourly mean speeds and gust speeds, maximum values likely to be exceeded only once in 10, 20, 50 and 100 years at 66 anemograph stations.

50s. (by post 52s.)

Published by

HER MAJESTY'S STATIONERY OFFICE

and obtainable from the Government Bookshops in London (post orders to P.O. Box 569, S.E.1), Edinburgh, Cardiff, Belfast, Manchester, Birmingham and Bristol or through any bookseller

METEOROLOGICAL OFFICE Met.O.816

THE METEOROLOGICAL MAGAZINE

Vol. 98, No. 1167, October 1969

551.525.2:625.7

NIGHT MINIMUM TEMPERATURES AT OR NEAR VARIOUS SURFACES

By W. G. RITCHIE

Summary. Minimum temperatures were obtained over the period October 1967–September 1968 at Wyton for thermometers in contact with concrete and with bitumen-covered concrete. The differences were small and the lower reading was taken as 'road minimum' and found to be generally higher than the minimum over grass and slightly higher than the minimum over bare soil.

Readings from two concrete sites and from two grass sites showed that the concrete (or road) minimum temperatures were less erratic spatially than the grass minimum temperatures.

The daily values of air minimum minus road minimum were found to be dependent on the length of night from sunset to sunrise. In winter the daily values were always within 2 degC of the curve fitted to the observed depressions of road minimum below air minimum.

No useful results were obtained from readings of a thermometer whose bulb was 2 inches below the concrete surface.

Purpose of the investigation. For a great many years it has been standard meteorological practice to expose a grass minimum thermometer nightly on a lawn of short grass between 1 in and 2 in above the ground and in contact with the tips of the grass blades.[1] The results are used mainly for forecasting ground frost over grassland, but forecasters are also required to predict frost on roads and runways, and no comparable measurements have been taken as a routine over surfaces of this kind. Indeed very little is known about minimum temperatures over concrete and how they compare with corresponding measurements over grass. An experiment was therefore set up in an open exposure on the airfield at Wyton, Huntingdonshire, in an attempt to increase our knowledge of this subject, and this paper reports the results of the first year's observations from October 1967 to September 1968.

Comparison of grass minimum temperatures at neighbouring sites. One question which must be asked is: What is the order of accuracy of a grass minimum temperature and what is the standard deviation between the readings of two grass minimum thermometers exposed a short distance apart on a flat grass surface? To answer this question two identical grass minimum thermometers were exposed nightly in open exposures on a flat sward 30 yards apart. Thermometer A was the thermometer in the enclosure and thermometer B was set up specially for this experiment. Monthly mean values of (A – B) and standard deviations in degC are given in Table I. (Tables I–V appear together overleaf.)

TABLE I — COMPARISON OF GRASS MINIMUM TEMPERATURES AT NEIGHBOURING SITES A AND B

	Oct.	Nov.	Dec.	Jan.	Feb.	Mar.	Apr.	May	June	July	Aug.	Sept.	Year
							degC						
Monthly mean (A – B)	+0·4	−0·4	−0·7	−0·7	−1·1	−0·5	−0·8	−0·7	−0·4	−0·3	+0·2	0·0	−0·4
Standard deviation	0·7	0·9	0·6	0·7	0·8	0·7	1·2	0·9	0·8	0·8	0·6	0·7	0·9

TABLE II — COMPARISON OF MINIMUM TEMPERATURES AT BITUMEN-COATED AND PLAIN CONCRETE SURFACES

	Oct.	Nov.	Dec.	Jan.	Feb.	Mar.	Apr.	May	June	July	Aug.	Sept.	Year
							degC						
Monthly mean*	+0·1	0·0	0·0	+0·1	+0·1	+0·3	−0·2	−0·2	−0·4	−0·4	−0·3	−0·1	−0·1
Standard deviation	0·3	0·3	0·4	0·3	0·3	0·4	0·3	0·2	0·3	0·4	0·3	0·3	0·4

* of plain concrete minimum temperature – bitumen-coated concrete minimum temperature

TABLE III — MONTHLY MEAN DIFFERENCES BETWEEN ROAD MINIMUM TEMPERATURES AND BARE SOIL MINIMUM TEMPERATURES

	Oct.	Nov.	Dec.	Jan.	Feb.	Mar.	Apr.	May	June	July	Aug.	Sept.	Year
							degC						
Mean*	+0·7	+0·2	+0·3	+0·2	0·0	+0·7	+1·8	+1·5	+1·8	+1·3	+0·7	+1·5	+0·9
Standard deviation	0·4	0·5	0·8	0·4	0·4	0·8	1·0	0·6	0·9	1·0	0·6	0·9	1·0

* of road minimum temperature – bare soil minimum temperature

TABLE IV — MONTHLY MEAN DIFFERENCES BETWEEN ROAD MINIMUM TEMPERATURES AND GRASS MINIMUM TEMPERATURES

	Oct.	Nov.	Dec.	Jan.	Feb.	Mar.	Apr.	May	June	July	Aug.	Sept.	Year
							degC						
Mean*	+1·7	+1·3	+0·9	+0·9	+1·4	+1·7	+2·8	+2·3	+2·7	+2·2	+1·1	+1·5	+1·7
Standard deviation	0·8	1·1	0·6	0·8	0·9	1·1	1·2	1·3	1·2	1·5	0·9	0·9	1·2

* of road minimum temperature – grass minimum temperature

TABLE V — MONTHLY MEAN DIFFERENCES BETWEEN AIR MINIMUM TEMPERATURES AND ROAD MINIMUM TEMPERATURES

	Oct.	Nov.	Dec.	Jan.	Feb.	Mar.	Apr.	May	June	July	Aug.	Sept.	Year
							degC						
Mean*	+1·2	+1·1	+1·8	+1·4	+1·0	+1·3	0·0	−0·6	−0·7	−0·8	−0·2	+0·2	+0·5
Standard deviation	0·5	0·9	0·6	0·8	0· 7	0·7	0·9	0·9	1·2	0·9	0·7	0·7	1·2

* of air minimum temperature – road minimum temperature

The graph of frequency of occurrence of values of (A – B) together with the normal frequency distribution curve for a standard deviation of 0·9 and 358 observations (8 observations were missed) are shown in Figure 1. The distribution is not normal for values of (A – B) within 0·8 degC of the mean, and this range includes 72 per cent of the cases. The seasonal variation was statistically significant at the 1 per cent level. The differences are thought to be due to the slightly different exposures, A being a little more open than B, and to differences in the grass. For the rest of this paper the readings of the thermometer outside the instrument enclosure have been used as the grass minimum temperatures because this thermometer is close to those on the concrete.

Method of exposure of thermometers on the various surfaces. It is not easy to measure the temperature of a surface. Robinson[2] exposed a grass minimum thermometer directly on close-cut grass and concluded that the surface behaved like a black body radiating at the temperature shown by the thermometer. On this basis it was decided to expose grass minimum thermometers resting with the bulbs in contact with the various surfaces and to assume that they would give the minimum temperatures of the surfaces. Figure 2 is a sketch plan of the site showing the positions of the thermometers.

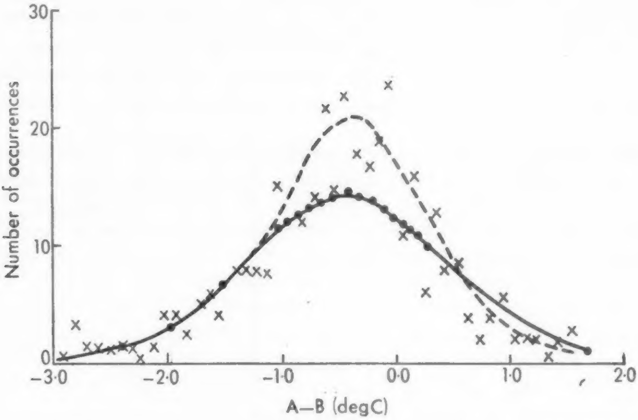

FIGURE 1 — DISTRIBUTION OF THE DIFFERENCES BETWEEN TEMPERATURES AS MEASURED BY TWO GRASS MINIMUM THERMOMETERS

x – – – – – x number of occurrences of values of A – B
· ———— · normal frequency distribution curve

All thermometers other than the grass minimum thermometers were resting on the surface with the bulb in contact with the surface. The top ends of the thermometers were inserted in strips of wood four inches long; this tilted the thermometers slightly and kept the bulbs in contact with the surface and also prevented rolling. All thermometers except number 5 are minimum thermometers. The positions of the thermometers are as follows:

Minimum thermometer 1 : At the centre of the signal square which is made of concrete 6 inches thick and is painted at least once a year with a thick coat of black bituminous paint. The sides of the square are 30 feet and the nearest side is 66 feet from the control tower which is the nearest building.

Minimum thermometer 2 : At the centre of the strip of concrete which was separated from the signal square by 24 feet of grass. The concrete is 6 inches thick and 24 feet wide.

Minimum thermometer 3 : A grass minimum thermometer conveniently supported at the centre of the grass strip and in line with thermometers 1 and 2.

Minimum thermometer 4 : At the centre of a 3-foot square patch of bare soil near the middle of the grass strip.

Thermometer 5 : A 2-inch bent-stem thermometer embedded in mortar in a crack in the centre of the concrete strip.

It was necessary to protect each thermometer from accidental damage without appreciably affecting the exposure of the ground to the night sky. The protection consisted of a framework of angle-strip aluminium (1/10 in thick, 1/2 in wide) in the form of an open 2-ft square with a 2-ft leg at each corner (see Figure 3).

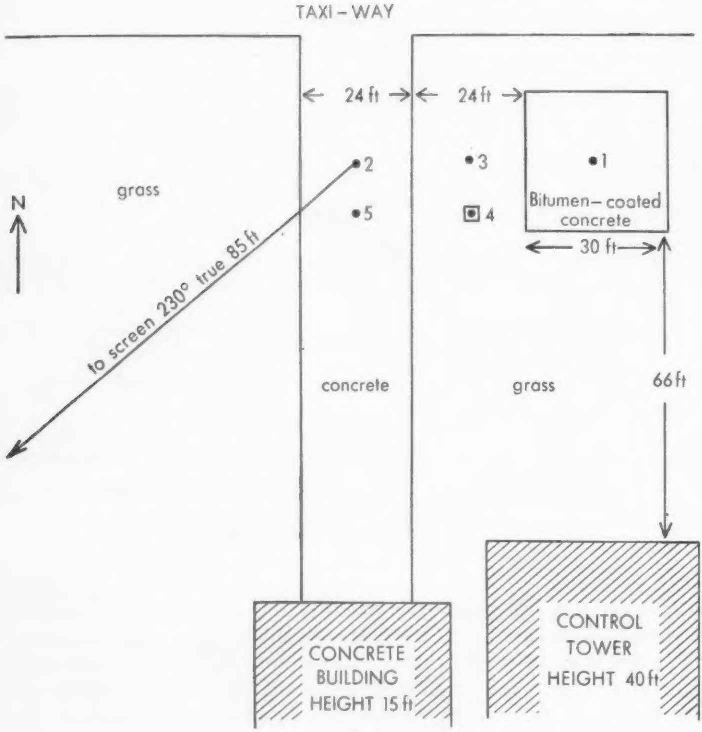

FIGURE 2 — PLAN OF SITE

1 = Minimum thermometer on bitumen-coated concrete
2 = Minimum thermometer on concrete
3 = Minimum thermometer on grass
4 = Minimum thermometer on bare soil
5 = 2-inch bent-stem thermometer in concrete

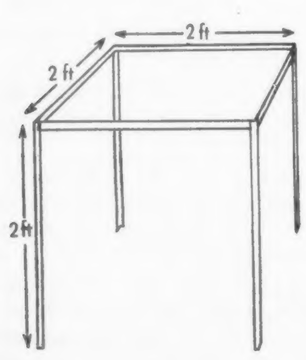

FIGURE 3 — THERMOMETER PROTECTION

The base of each leg, over concrete and tarmacadam, was inserted into a piece of lead piping about 2 inches long to prevent movement by wind. The thermometer was arranged so that the bulb was centrally placed beneath the framework.

Thermometers 1 to 4 were read at 09 GMT and thermometer 5 at 12 GMT.

Comparison of minimum temperatures at two concrete surfaces 300 yards apart. For reasons unconnected with the experiment it was necessary to transfer minimum thermometer 2 to another piece of concrete at the end of the year. Concrete minimum temperatures were read at both sites from 1 June till 30 September 1968. The standard deviation of the differences was 0·4 degC. The standard deviation of the differences between two grass minimum temperatures (Table I) for the same period was 0·8 degC. The standard deviation of the differences of the concrete minimum temperature was thus only half that of the differences between the grass minimum temperatures, even though the 'concrete' thermometers were much farther apart. Dight (personal communication) obtained a similar result at Edinburgh/Turnhouse.

Comparison of minimum temperatures at bitumen-coated and plain concrete surfaces. Monthly mean values and standard deviations of plain concrete minimum temperature minus bitumen-coated concrete minimum temperature are given in Table II. This shows that minimum temperatures were slightly lower at the bitumen-coated surface from October to March, and slightly lower at the plain concrete surface from April to September. These differences are smaller than had been expected in view of the different colours of the surfaces. The distribution of the differences between plain concrete and bitumen-coated concrete minimum temperatures is shown in Figure 4. The distribution differs from a normal distribution in the

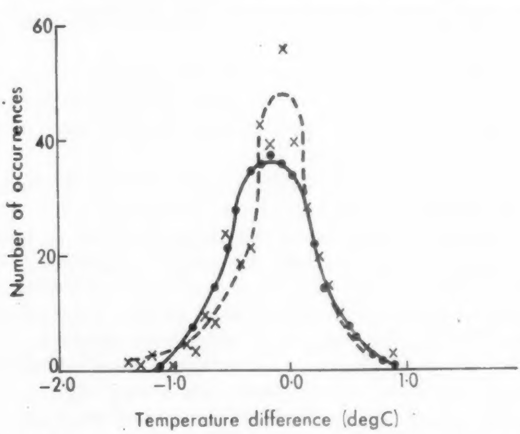

FIGURE 4 — DISTRIBUTION OF THE DIFFERENCES BETWEEN MINIMUM TEMPERATURES ON PLAIN CONCRETE AND THOSE ON BITUMEN-COVERED CONCRETE

x – – – – x number of occurrences
· ———— · normal frequency distribution curve

range +0·1 degC to −0·2 degC and this includes half of the cases. As, however, the differences are so small and the number of very small differences is above average, it seems reasonable to assume that minimum temperatures at these two surfaces can be considered to be the same. The lower of these temperatures is called the 'road minimum temperature' for the rest of this paper.

Minimum temperatures over bare soil. Figure 2 shows that the thermometer on bare soil was between the 'concrete' thermometers and in line with them. Monthly mean values of road minimum temperature minus bare soil minimum temperature are given in Table III. From March to October the road minimum temperature was almost always higher than the bare soil minimum temperature; from November to February the road minimum temperature was lower on 28 per cent of occasions. The seasonal variation was statistically significant at the 1 per cent level.

Comparison of road minimum temperature and grass minimum temperature. The road minimum temperature was higher than or equal to the grass minimum temperature on 96 per cent of occasions. Monthly mean values of road minimum temperature minus grass minimum temperature are given in Table IV. The largest value was 6·0 degC in April.

Depression of road minimum temperature and grass minimum temperature below air minimum temperature. Monthly mean values of air minimum temperature minus road minimum temperature are given in Table V; daily values are shown on the upper part of Figure 5. The curve-fitting was confirmed by computer. A Fourier analysis showed that the curve was closely represented by a simple sine curve, the harmonics being negligible.

The equation is:

$$y = 0{\cdot}48 + 1{\cdot}22 \sin x$$

where y is the depression in degC and x is the day as an angle assuming 365 days = 360°.

The largest departures from the curve occurred in the summer months. For the purpose of forecasting ice on roads and runways the daily values between November and March were always within 2 degC of the curve and on most occasions within 1 degC of it.

Parrey[3] took road minimum temperatures at Watnall during the winter months in 1967–68 and he concluded that 'for a given road, the depression of the road temperature at night below the air temperature at four feet depends largely on the length of time available for outgoing radiation'; he showed this diagrammatically by superimposing a curve of the duration from sunset to sunrise on the annual trend of depression of road minimum temperature below air minimum temperature. The length of night from sunset to sunrise at 52°N is drawn in the lower part of Figure 5. It fits the curve of air minimum temperature minus road minimum temperature with a very slight lag and strongly supports Parrey's conclusion. J. S. Hay[4] considered road and air minimum temperatures on the M1 motorway near Newport Pagnell and on a slip road off the M4 motorway near Bray Wick. He found smaller mean values of air minimum temperature minus road minimum temperature, but larger extreme values.

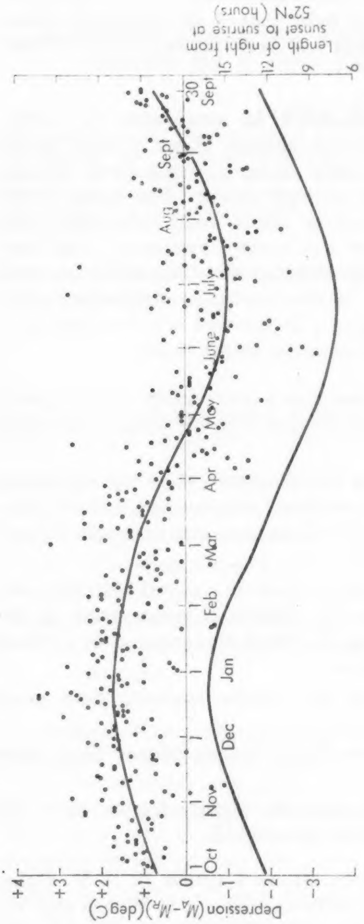

FIGURE 5—DEPRESSION OF ROAD MINIMUM BELOW AIR MINIMUM TEMPERATURE (UPPER CURVE) COMPARED WITH LENGTH OF NIGHT (LOWER CURVE)

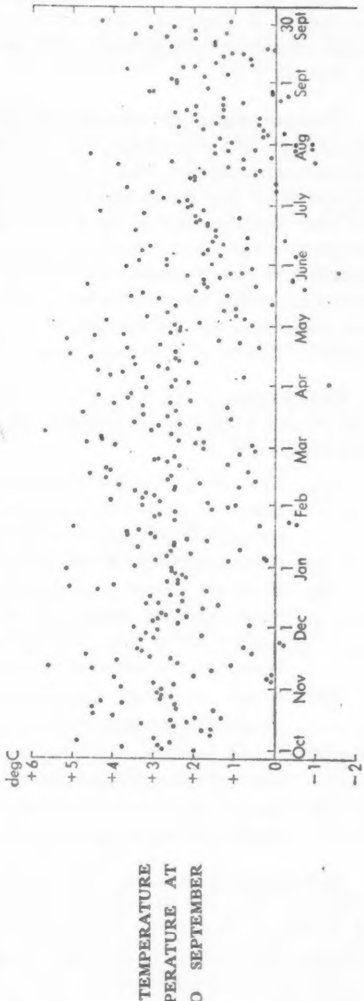

FIGURE 6—AIR MINIMUM TEMPERATURE MINUS GRASS MINIMUM TEMPERATURE AT WYTON—OCTOBER 1967 TO SEPTEMBER 1968

Daily values of air minimum temperature minus grass minimum temperature are shown in Figure 6. The scatter is about twice that of air minimum minus road minimum temperature and no attempt has been made to draw a line of best fit.

Temperature of thermometer embedded in concrete. In winter at 12 GMT this temperature is usually (but not always) about 2 degC below the air temperature. In summer it is usually about 3 degC above the air temperature but on sunny days it can be 10 degC above. The value of the 12 GMT temperature from within the concrete minus road minimum temperature read next morning shows large day-to-day variations — on one occasion it was 23 degC. No useful relationship between this difference and cloud and wind has yet become apparent. In the next stage of the experiment thermometers will be embedded at depths of 4 inches and 8 inches, and it is hoped that one of these will be at a depth to give a useful result.

Conclusions. As far as the results of one year's observations at one place can be considered to be of more general application, the following conclusions are suggested:

(i) The depression of road minimum temperature below air minimum temperature is a function primarily of date, and can be obtained from a graph (Figure 5) to within 1 degC in most cases and to within 2 degC in all cases during the winter.

(ii) Whether a road is made of concrete or concrete covered with bitumen seems to have very little effect on the minimum temperature at the surface. The two pieces of concrete on which this conclusion is based both had the same vertical thickness.

(iii) Road minimum temperatures are less erratic spatially than grass minimum temperatures.

(iv) Road minimum temperatures are almost always higher than grass minimum temperatures.

(v) Road minimum temperature is normally slightly higher than the minimum temperature at the surface of bare soil.

Acknowledgements. The author thanks Group Captain D. S. V. Rake, O.B.E., A.F.C. for allowing the experiment to be carried out at Wyton and Mr S. E. Virgo, O.B.E. for helpful advice and criticism. He also thanks the Fire Section for cheerfully putting themselves to considerable inconvenience in avoiding the thermometers, and the staff of the Meteorological Office for willingly taking these non-standard observations.

REFERENCES

1. London, Meteorological Office. Observer's Handbook, Third Edition. London, HMSO, 1968, p. 180.
2. ROBINSON, G. D.; Notes on the measurement and estimation of atmospheric radiation. *Q. Jnl R. met. Soc., London*, 73, 1947, p. 127.
3. PARREY, G. E.; Minimum road temperatures. *Met. Mag., London*, **98**, 1969, p. 286.
4. HAY, J. S.; Some observations of night minimum road temperatures. *Met. Mag., London*, **98**, 1969, p. 55.

551.521.14(427)

A DETERMINATION OF THE ALBEDO OF MORECAMBE BAY NORTH OF A LINE FROM ALDINGHAM TO BARE

By V. C. BENDELOW

Summary. Aerial photographs of Morecambe Bay were taken during low-tide situations in 1964 and 1967. Each photographic frame was divided into areas of ground-shade types based on photographic tone and the appearance of the surface texture. Ground measurements of albedo were made for each shade type and mean values obtained, from which an overall mean albedo of about 14 per cent was calculated for the area of Morecambe Bay under examination.

Introduction. In this study albedo, expressed as a percentage, is defined by the equation

$$A = \frac{I_r}{I_0} \times 100,$$

where I_r is the solar energy reflected by the surface and I_0 is the solar energy incident on the same surface for wavelengths in the region of 0·3 to 3·0 microns.

There were three main parts to the investigation:

(i) The production of maps showing areal distributions of albedo in terms of ground shades on aerial photographs.

(ii) The measurement (from the ground) of the albedo of each ground-shade type.

(iii) The calculation of a mean value of the albedo for Morecambe Bay in a low-tide situation, using the values found in the previous two sections.

Method. The production of areal shade distribution maps was from aerial photographs of Morecambe Bay taken during low-tide situations. The limits of the area studied were taken as north of a line from Aldingham to Bare and the high-water mark on the coast, this being an area largely exposed at low tide (see Figure 1). High water extends the limit up the river Kent as far as Sampool Bridge and up the river Leven as far as Haverthwaite.

The possibility of using aerial photographs to estimate the albedo of the ground was first suggested and tested by Dr F. K. Hare and Dr S. Orvig in 1962.[1] They pointed out that those areas reflecting a high percentage of the incident radiation (high albedo) would appear light on aerial photographs. Similarly, areas of low albedo would appear dark. They also suggested that if the exact conditions of film, printing paper, exposure, development and printing were known, it should be possible to relate photographic shade to albedo. However, aerial photographs may appear to have the disadvantage, from the point of view of albedo studies, of being taken with a minus blue filter and of spanning only that part of the spectrum from 0·5 to 0·68 micron. Later investigation by Hare and Orvig showed that this comparatively narrow range of wavelengths is no great disadvantage.

Using this method, two ground-shade distribution maps for Morecambe Bay for the periods August 1964 and July to September 1967 were constructed from aerial photographs. In 1964 the photographs were taken at an altitude

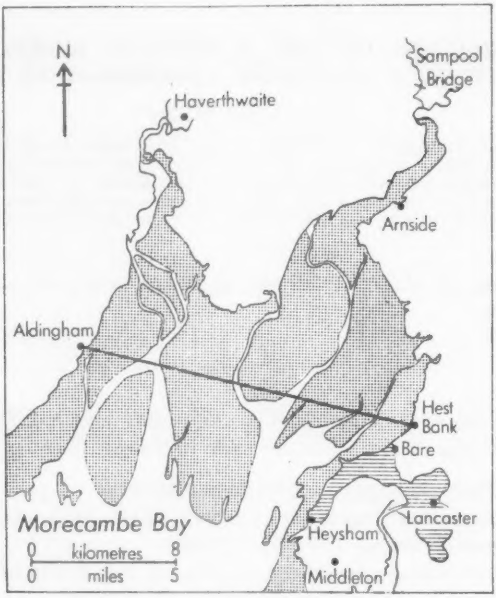

FIGURE 1 — THE MORECAMBE BAY AREA
The shaded part represents the extent of the sand which is exposed at low tide, and the hatching represents built-up areas.

of 10 000 ft on two consecutive days in August. In 1967 the altitude was 6000 ft and the photographic runs were made on six separate days. The method consisted of taking each photographic frame and dividing it up into ground-shade types, of which there are five.[2] The sub-division into types was based on photographic tone (using the Kodak grey scale) and appearance of the surface texture (using a stereoscope).

Since each aerial photograph overlaps the next in the run by 60 per cent, all areas of sand could be viewed on three consecutive frames. Also each run overlaps the adjacent run by 20 per cent, therefore areas within a 20 per cent border strip could be further checked with the adjacent photographic run.

Plate V shows an aerial photograph, taken at low tide, which has been divided into shade types to demonstrate the sub-divisions listed in Table I. The variation from the darkest to the lightest tones between the low and high water marks respectively is clearly seen, but the fact that the different shade types are clearly delineated suggests that the water content of the sand does not vary smoothly between high and low water mark.

Shade type (4) is clearly defined by the water's edge, while the line of demarcation between type (2) and type (3) may be related to the position of the water table. Shade type (1) was readily identified with salt marsh areas (using a stereoscope) while shade type (2 + 3) was associated with gulleys and streams.

TABLE I — SHADE TYPE SUB-DIVISIONS

Shade type	Surface texture	Grey scale number
(1)	Salt marsh	0·75–1·25
(2)	Dry sand	0·00–0·10
(3)	Wet sand	0·40–0·55
(4)	Water	0·75–1·00
(2+3)	Dry sand crossed by wet sand lattice*	0·00–0·55

*Dry sand crossed by a network of shallow streams giving the appearance of dark strips against a lighter base. These are not to be confused with ripples in uniform sand where the dark lines are shadows cast by the crests of the ripples.

Attempts to measure the albedo of each shade type from an aircraft flying at 200 ft (61 m) proved to be unsuccessful with the equipment and time available. The main calibration therefore had to be confined to measurements on the ground.

Ground measurements were taken using two solarimeters, one facing upwards and the other facing downwards, mounted on opposite ends of a horizontal bar a few feet above the ground and supported on a tripod. The readings were taken at Heysham, Middleton and Hest Bank at various positions along lines at right angles to the coast, all within a quarter of a mile of a central point for each shade type. Readings for shade (2 + 3) were limited to a transect down a gulley.

A mean albedo for the Bay was found by measuring the cumulative area of each shade type on both the 1964 and 1967 maps (using a planimeter) and assigning to each area the corresponding measured value of albedo. From these data an overall mean value of albedo was obtained for the Bay, north of a line from Aldingham to Bare, for low-tide situations.

Results. The results are summarized in Table II, showing the shade type distribution, and in Table III, showing the corresponding albedo values.

TABLE II—SHADE TYPE DISTRIBUTION

	1964		1967	
Shade type	Map area *cm²*	Fraction of total area *per cent*	Map area *cm²*	Fraction of total area *per cent*
(1)	404	8	600	4
(2)	434	9	606	4
(3)	1 468	30	8 932	52
(4)	584	12	1 755	10
(2+3)	1 972	41	5 071	30
Totals	4 862*	100	16 964*	100

*The difference in total map area is due to different map scales as the 1967 aerial photographs were taken at a lower altitude.

TABLE III—MEASURED VALUES OF ALBEDO

Shade type	Albedo (mean) *per cent*	Standard deviation *per cent*	Number of observations
(1) Salt marsh	15·7	2·4	20
(2) Dry sand	35·4 dry surface	1·3	19
	17·0 damp surface	1·9	22
(3) Wet sand	15·9	1·8	21
(4) Water	10·8	0·4	16
(2+3) Lattice	12·7	0·8	10

Discussion of results.

Results for areas of different shade types. The two values of albedo given for shade type (2) require some explanation. In practice, sand areas of type (2) may embrace a wide range of surface moisture conditions. Under the driest conditions, when a greater proportion of the incident radiation is reflected, the albedo has a comparatively high value of about 35 per cent. But when sand of the same shade type and therefore of similar superficial appearance has a damp surface, less energy is reflected and the albedo has the much lower value of 17 per cent. This value may be compared with that obtained for shade type (3), i.e. wet sand, for which the albedo is about 16 per cent.

Presumably therefore, if the water content of sand of shade type (2) were progressively increased it would ultimately change its appearance from that of type (2) to that of type (3). This change in appearance is not however accompanied by much appreciable change in the albedo (17 per cent to 15·9 per cent, Table III).

Although a gradual transition in appearance from type (2) to type (3) areas may have been expected, the aerial photographs obtained show quite clearly that the change in appearance is quite abrupt. It is suggested that the well-defined boundary between sand of these two types is associated with the water table.

Since areas of shade type (2) with a damp surface have an albedo which does not differ appreciably from areas of shade type (3), it is convenient, under damp conditions, to group these two shade types together and attribute to them a mean value for the albedo of $16 \cdot 5 \pm 2$ per cent. This then is the value that could be expected from both shade types during periods of prolonged rainfall or when low tide occurs in the early morning or late evening. It could even possibly apply during most of the winter months.

The lower value of 12·7 per cent for surface areas of type (2+3), i.e. 'dry' sand covered by wet sand lattice, can be explained satisfactorily by the fact that little, if any, of this type of surface is likely to be completely dry and that there will almost certainly be some surface water present which will absorb a greater proportion of the incident radiation.

A 'Student's' *t*-test carried out on these results showed that type (2) (damp surface) and type (3) probably belong to the same population whereas type (2+3) does not.

Finally, a comparison may be made between the mean albedo value of 10·8 per cent obtained for areas of shade type (4), i.e. water-covered areas at low tide, and the mean value for water alone, i.e. 8 per cent. The higher value of 10·8 per cent corresponds to turbid water near the shore. Thus for water under conditions of high turbidity in a shallow sandy estuarine area a higher value of albedo is obtained than for areas of deep water. It would be particularly interesting to know the precise value of albedo for the whole area at high tide, to compare its value with the known value for deep water, and also to investigate its variation (if any) with the depth of water in the Bay.

Results for the whole area. The value for the effective albedo for the whole area for low-tide situations in August 1964 and July–September 1967 may be summarized as follows:

(i) Under dry conditions, with albedo value 35·4 per cent for shade type (2) :
Mean overall albedo 1964 : 15·5 per cent.
Mean overall albedo 1967 : 15·1 per cent.

(ii) Under wet conditions, grouping shade types (2) damp and (3) together and allocating an albedo of 16·5 per cent :
Mean overall albedo 1964 : 14·0 per cent
Mean overall albedo 1967 : 14·3 per cent.

Thus in spite of differences between 1964 and 1967 in the tidal situations and in the areal extent of the different shade types, and in spite of a variation in albedo for shade type (2) from about 16 per cent to 35 per cent, the overall albedo appears to have remained more or less unchanged in both dry and damp conditions.

Further problems. It is satisfactory to note the general agreement between the results obtained for 1964 and for 1967. Nevertheless, the study poses several interesting problems that deserve further investigation; for example, the precise effect of moisture on areas of shade type (2), the reasons for the abrupt changes in appearance between different shade types (especially types (2) and (3)), the diurnal and seasonal variations of albedo, and the influence of atmospheric conditions.

Acknowledgements. The author wishes to thank the Meteorological Office for the loan of necessary equipment, Messrs C. S. Allcott and Son for permission to reproduce part of an aerial photograph and Hunting Survey for the supply of the photograph; also Professor Gordon Manley (University of Lancaster) and Mr A. S. Edmondson, M.Sc., (Royal Holloway College, University of London) for valuable discussion during the preparation of this paper.

REFERENCES

1. MORRISON, A.; Relation between albedo and air photographic tone in Canadian sub-arctic regions. *Canadian Geographer, Manotick*, **8**, 1964, p. 272.
2. DAVIES, J. A.; Albedo measurements over sub-arctic surfaces. *McGill sub-arct. Res. Pap., Montreal*, 1962, No. 13.

551.509.312:551.543.5

FORECASTING THE MOVEMENT OF ISALLOBARS INTO EASTERN ENGLAND

By J. M. NICHOLLS and G. A. CORFIELD

Summary. A method is given of forecasting pressure falls of 4 mb or more in 3 hours in eastern districts of England. The method utilizes Petterssen's kinematic rules to calculate the speed of a – 4-mb isallobar which has already appeared in some other area of the British Isles. A more usual method of calculating isallobaric speed is by following the movement of the isallobar on successive hourly charts. The advantage of the procedure described below over the 'chart-to-chart' method is that it enables a forecast to be issued earlier.

Introduction. Forecasts of pressure falls greater than 4 mb in 3 hours are required by some collieries in the U.K. owing to the association between these pressure falls and the expansion of large stagnant reservoirs of methane gas in waste areas of a mine, the gas at times overflowing into the ventilation system and working areas of the mine.[1]

Forecasting of large pressure falls is thus an integral part of the work of the forecaster at some outstations, and a quick method of forecasting these falls from available synoptic charts was needed. Since 3 hours' notice of the start of a fall of 4 mb in 3 hours is required by the collieries, warnings should ideally be issued at least 6 hours before the arrival of the – 4-mb isallobar.

Special reference is made in this paper to north-east England since there is a requirement to forecast falls for collieries in that area. The method to be described can, however, be applied to all eastern and Midland areas of England. Forecasting for these areas is made comparatively easy since most systems associated with large pressure falls are eastward-moving depressions, troughs, or fronts, and the falls first appear in western areas.

The kinematic method of calculating isallobaric speed. The speed of movement of an isallobar in the direction of movement of an isallobaric low is given by Petterssen[2] as

$$C = - \frac{\dfrac{\partial}{\partial t}\left(\dfrac{\partial p}{\partial t}\right)}{\dfrac{\partial}{\partial x}\left(\dfrac{\partial p}{\partial t}\right)} \qquad \ldots (1)$$

Now $\dfrac{\partial}{\partial t}\left(\dfrac{\partial p}{\partial t}\right)$ represents the local change with time of the pressure tendency, and can therefore be evaluated as a finite difference from two consecutive hourly charts. Also $\dfrac{\partial}{\partial x}\left(\dfrac{\partial p}{\partial t}\right)$ can be evaluated as a finite difference, since it represents the change in pressure tendency with distance along a line parallel to the direction of movement of the isallobaric low and through the areas in question. An approximation to this direction is given by the line of movement of the system associated with the pressure falls or the direction of the warm-sector isobars as seen on the latest 3-hourly North Atlantic chart.

The time at which a pressure fall of 4 mb in 3 hours will start in area A is deduced from equation (1) as follows:

(i) Watch for the hourly chart on which the – 4-mb isallobar first appears, and on this GG chart (GG representing the time of the chart to the nearest hour GMT) draw the – 3-mb and – 4-mb isallobars, in that order, as smooth lines (Figure 1(a)).

(ii) Note the average change in tendency (i.e. tendency at GG minus tendency at (GG – 1)), at stations near this line, for stations which 'fitted' the – 4-mb isallobar on the GG chart. Let 'q' be the negative of this value (Figure 1(b)).

PLATE I—SKUA TEAM, GAN 1968

Front row: Cpl C. Atkinson, W/O C. G. Smith, Mr R. Almond, Dr R. Frith, W/O D. S. Monk, Cpl A. Houseman.

Back row: Mr D. E. Warner, Mr R. J. Shearman, Sgt F. Brumby, Sgt G. Hayward

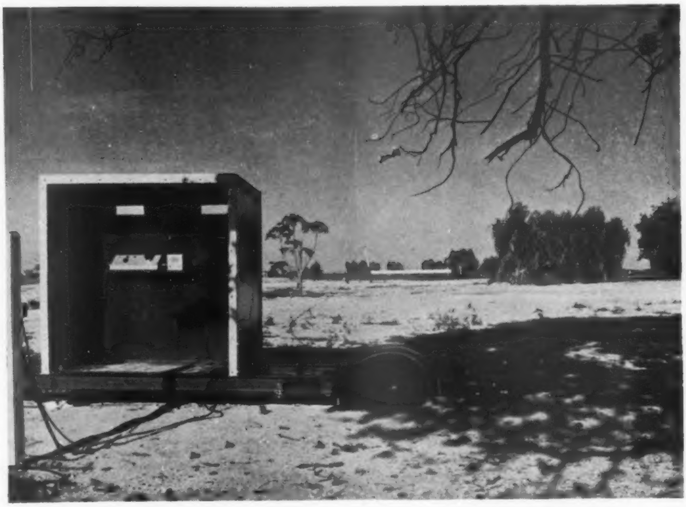

PLATE II—FIRING POINT WITH LAUNCHER PAD IN BACKGROUND

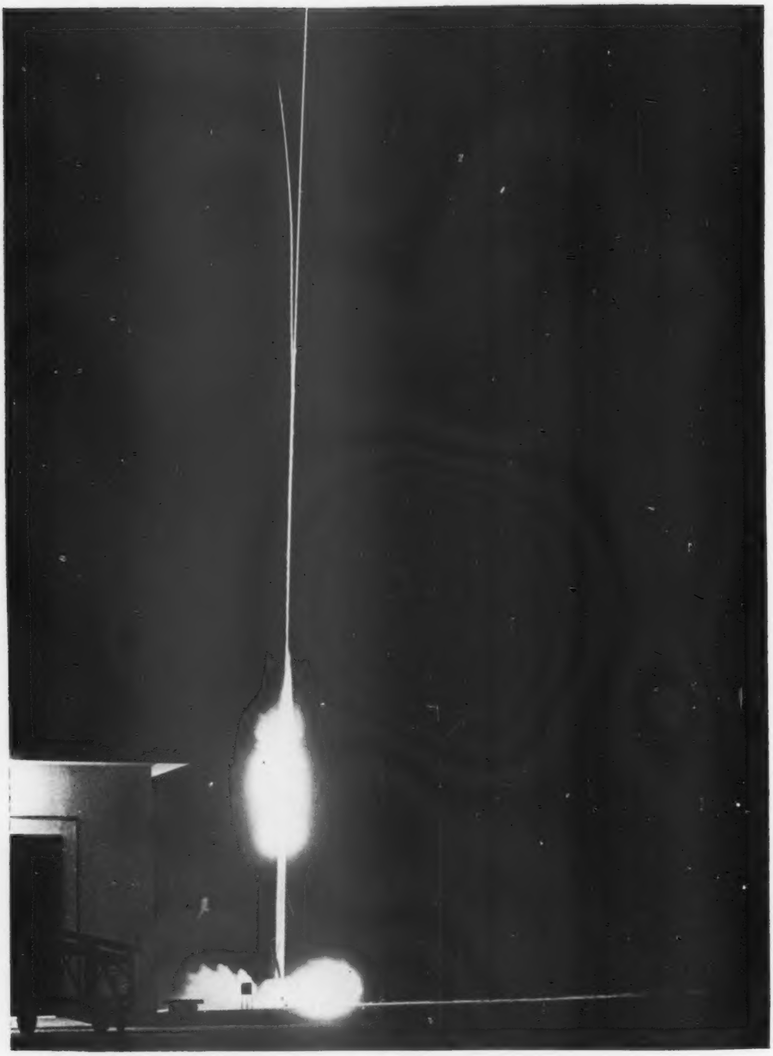

PLATE III—SKUA ROCKET LAUNCH, GAN

Time-lapse photograph shows the rocket path as a straight streak of light. The curved streak to the left is the detachable first stage or boost motor, which falls away and descends attached to a parachute.

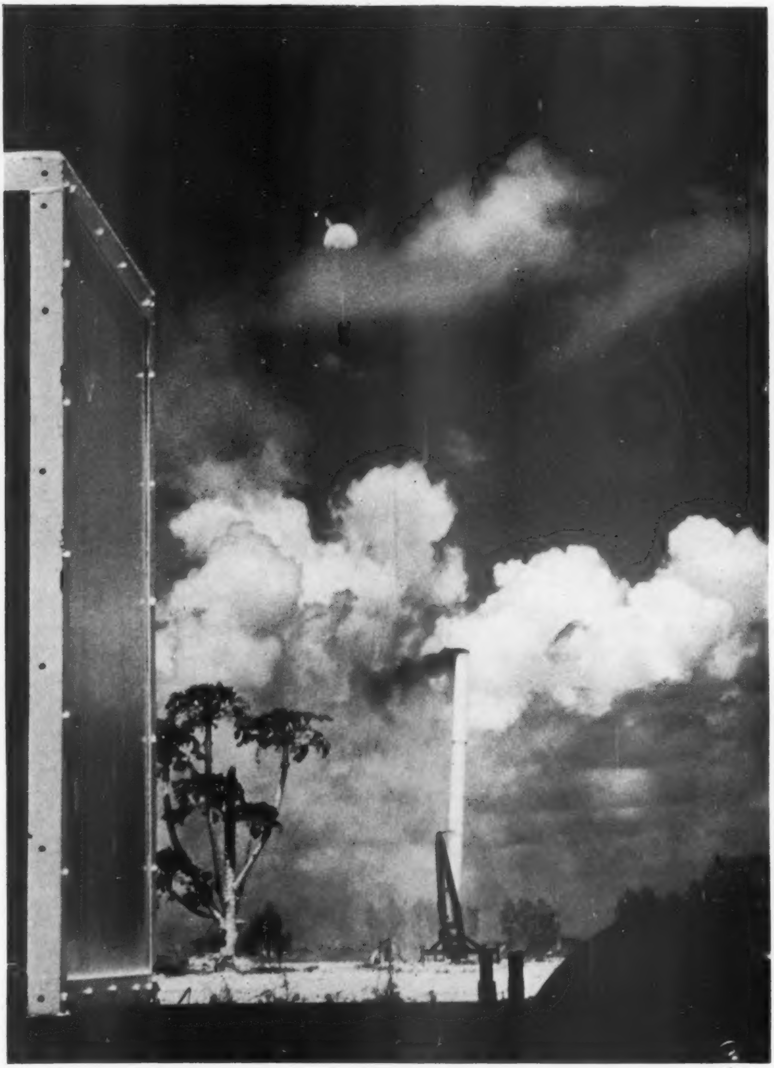

PLATE IV—BOOST MOTOR DESCENDING ATTACHED TO A PARACHUTE AFTER DAYLIGHT LAUNCH FROM GAN

Photograph by courtesy of Hunting Surveys

PLATE V—AN AERIAL PHOTOGRAPH TAKEN OVER THE RIVER KENT AT ARNSIDE AT AN ALTITUDE OF 10 000 FT, AUGUST 1964.

The photograph has been divided up into shade types as an illustration of the method. See page 306.

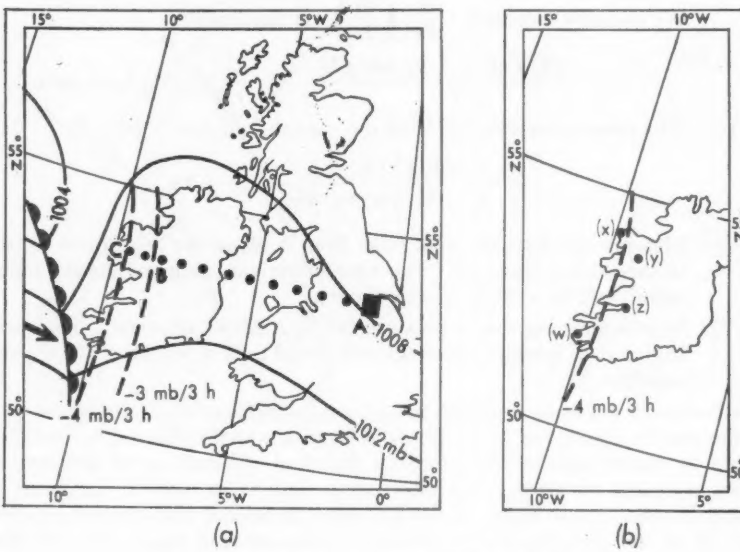

FIGURE 1 — CALCULATION OF SPEED OF ISALLOBARS

(a) Chart GG from which r and x are obtained
— — — isallobars
———— isobars

Heavy arrow shows direction of movement of system. Dotted line ABC is drawn through area A parallel to this arrow and intersects the – 4-mb/3 h isallobar at C and the – 3 mb/3 h isallobar at B. Then BC = r and AC = x n. miles.

(b) Data from which q is obtained. The dashed line shows the position at time GG of the – 4-mb/3 h isallobar. At stations near this line the figures in brackets (represented by x, y, etc.) give the change in the 3-hourly tendency between chart GG and chart GG–1. Then q is obtained as an average of these changes.

We have now calculated $-\dfrac{\partial}{\partial t}\left(\dfrac{\partial p}{\partial t}\right)$ in the form:

$$-\left\{\left(\frac{\partial p}{\partial t}\right)_{GG}-\left(\frac{\partial p}{\partial t}\right)_{GG-1}\right\} = q \text{ (mb/3 h)/h.}$$

(iii) On the GG chart draw a line through A parallel to the direction of motion of the system associated with the falls, as deduced from the GG chart or from the latest 3-hourly chart. If this line does not intersect the – 4-mb isallobar, this fall is unlikely to occur in area A.

(iv) Measure the distance 'r' nautical miles (n. miles) between the intersections of this line with the – 4-mb and – 3-mb isallobars, on the GG chart, if these intersections exist.

We can now calculate $\frac{\partial}{\partial x}\left(\frac{\partial p}{\partial t}\right)$ in the form

$$\frac{-3\text{ mb/3h} - (-4\text{ mb/3 h})}{r} = \frac{1}{r}\ \text{(mb/3 h)/n. mile.}$$

(v) The speed of translation 'c' of the -4-mb isallobar is given by

$$c = \frac{q\ \text{(mb/3 h)/h}}{1/r\ \text{(mb/3 h)/n. mile}} = qr\ \text{kt.}$$

(vi) Measure the distance 'x' n. miles from A along the line drawn in (iii) to the -4-mb isallobar. The time of arrival, assuming steady translation, will be at (GG + x/qr) hours.

(vii) Issue a warning that a pressure fall of 4 mb or more in 3 hours will begin, at A, 3 hours before the calculated time of arrival of the -4-mb isallobar.

The forecaster will have to use his judgement in application of instruction (iii). If the system associated with the falls were a mobile depression, the line would be drawn parallel to its forecast direction of motion over the next 12 hours or to the direction of its warm-sector isobars as seen on the latest 3-hourly North Atlantic chart. If the falls were associated with a frontal system moving in the circulation of a distant or slow-moving depression, the line should be drawn parallel to the warm-sector isobars.

Collieries also require a separate warning of falls of or greater than 8 mb in 3 hours; the above methods could of course be used to predict falls of this magnitude for eastern areas.

Two examples illustrating the use of the method:

Figure 2. On 15 March 1965 a depression moved north-eastwards from 53°N 10°W at 06 GMT to 57°N 6°W at 18 GMT. The first appearance of the -4-mb isallobar on an hourly chart was at 07 GMT (Figure 2(a)) and by applying instruction (ii) the value of 'q' was found to be 0·8 (mb/3 h)/h (Figure 2(b)). The system associated with the falls was a frontal trough, as deduced from the 06 GMT North Atlantic chart. By drawing the line in (iii) parallel to the 06 GMT warm-sector isobars and through area A on the 07 GMT hourly chart the distance (r) between the intersections of this line with the -3-mb and -4-mb isallobars was found to be 45 n. miles. Thus the speed of the isallobar was $0{\cdot}8 \times 45 = 36$ kt. The distance away of the isallobar at 07 GMT was 300 n. miles giving an expected arrival time of 1515 GMT in area A. According to rule (vii) a warning could have been issued, based on the 07 GMT chart, that the pressure fall of 4 mb in 3 hours would start at 1215 GMT. The actual start of the fall of 4 mb in 3 hours was at 1300 GMT.

Figure 3. On 3 March 1965 there was a clear appearance of a -4-mb isallobar over western Scotland on the 00 GMT chart. The system associated with the falls was identified on the North Atlantic chart for 21 GMT on 2 March as a depression moving south towards Northern Ireland. A line drawn through area A on the 00 GMT chart parallel to the direction of motion of the depression would not cut the -4-mb isallobar and thus the evidence of the 00 GMT chart would not indicate a need for a warning of a fall of 4 mb in 3 hours in area A. Falls of 4 mb or more in 3 hours did not in fact occur in that area.

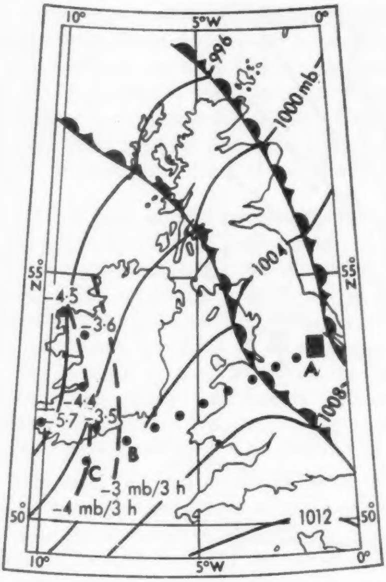

(a)

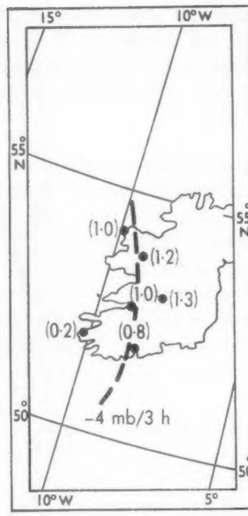

(b)

FIGURE 2 — CALCULATION OF TIME OF PRESSURE FALL OF 4 mb/3 h IN AREA 'A' ON 15 MARCH 1965

(a) Chart for 07 GMT 15 March 1965
— — — isallobars
——— isobars
Dotted line ABC is drawn through area A parallel to direction of movement of system and intersects isallobars at B and C. BC=45 n. miles; AC=300 n. miles.

(b) Data from which *q* is obtained for 15 March 1965. The dashed line shows the position of the −4-mb/3 h isallobar at 07 GMT. The figures in brackets give the change in 3-hourly tendency between 0600 and 07 GMT and the average of these figures over southern Ireland is 0·8 mb.

In cases such as this, however, it is advisable to maintain an hourly watch on the movement of isallobars and if possible on the movement of the system associated with the pressure falls.

The causes of error in the method. In deriving the kinematic method it was assumed that no redistribution of pressure tendencies occurs within the isallobaric low as it moves from the initial area of occurrence of large pressure falls to area A (see Figure 1), but such a redistribution can cause errors in the calculated time of arrival of the −4-mb isallobar and may be associated with three types of change. These are (i) change in the rate of deepening (or filling) of the associated pressure system, (ii) change in the speed

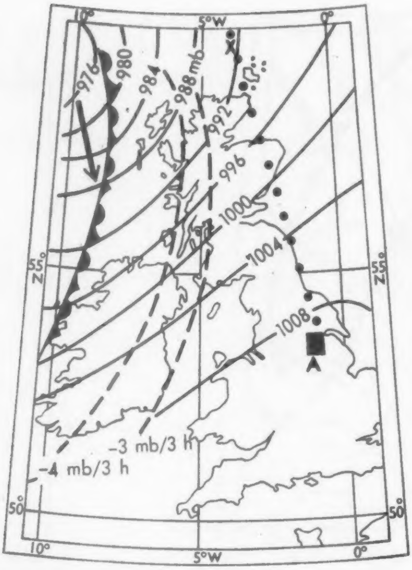

FIGURE 3 — EXAMPLE (00 GMT 3 MARCH 1965) WHERE FALLS OF 4 mb OR MORE IN 3 hours WERE NOT ADVECTED INTO AREA 'A'

— — — isallobars; ——— isobars.

Heavy arrow shows direction of movement of system. Dotted line AX is parallel to this direction and does not intersect the isallobars for – 4 mb/3 h or – 3 mb/3 h.

of the system, and (iii) change in the pressure gradients within the system during the calculated period of movement. It was also assumed that there would be steady linear translation of the isallobaric low to area A; thus errors in the calculated time of arrival may also arise because of a fourth type of change: namely, a change in the direction of movement of the associated pressure system.

The magnitude of these four changes which may contribute to errors would depend critically on the nature of the associated pressure system and the thermal flow in which it was embedded. For example one would expect all four changes to be small for a wave depression moving under a strong thermal gradient. However for a depression whose fronts are occluding the four changes would be greater in magnitude. It is worth while noting here, however, that a constant rate of deepening or filling is not associated with a change in the tendency distribution and therefore does not contribute to errors.

In association with the four types of change detailed in this section there will be an error in the calculated time of arrival of the – 4-mb isallobar. In order to deduce a correction to be applied to the time calculated, as above, by using a method based on kinematic rules, it would be necessary to forecast quantitatively these changes over the period of advection and deduce individual corrections dependent on each type of change. This would, however, be a difficult and time-consuming task for the forecaster.

The intensity of the isallobaric low may be changed by diurnal oscillations of pressure; these occur with a period of 12 hours, the times of greatest fall being between 10 and 16 LMT and between 22 and 04 LMT. The fall may be about 1 mb/3 h but varies according to the season.[3] It is difficult for the forecaster to take account of diurnal changes but they would obviously become of importance when falls originally near the warning limit were forecast to arrive in area A at times of maximum diurnal change.

Usefulness of the method. The only method previously in use of forecasting pressure falls of 4 mb or more in 3 hours was of following the movement of the −4-mb isallobar on successive hourly charts and thus deducing its speed. The accuracies of the forecast times of onset and the warning periods given by the 'chart-to-chart' method and the kinematic method were compared by using both methods, in retrospect, to forecast the start of pressure falls of 4 mb or more in 3 hours which had occurred over north-east England over a six-month period; the hourly U.K. charts and three-hourly North Atlantic charts were used strictly according to the prescribed methods, that is as they should have been used if forecasting in advance the onset of the falls.

Figures 4 *(a)* and *(b)* show the distribution of the number of hours warning given by each method for 49 cases of pressure falls of 4 mb or more in 3 hours, which occurred in the six-month period. '$T_4 - T_a$' and '$T_4 - T_b$' are the time differences between the actual time of onset 'T_4' of the pressure fall and the times of issue of the warning by the kinematic method (T_a) and 'chart-to-chart' method (T_b) respectively. The times of onset 'T_4' in the Newcastle and Doncaster areas were deduced from the Acklington and Finningley barograms. 'T_a' and 'T_b' are the times of the latest hourly chart used in each method plus $1\frac{1}{2}$ hours, which is added since the hourly chart is not available in the forecast office till $1\frac{1}{4}$ hours after the hourly observations and about $\frac{1}{4}$ hour is needed to use the methods. '$T_4 - T_a$' has an average value of 3 hours 35 minutes and '$T_4 - T_b$' an average value of 2 hours 50 minutes.

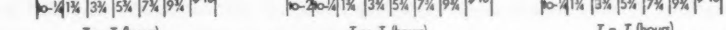

(a) Strict use of kinematic method (b) Strict use of chart-to-chart method (c) Method used by forecaster (see text)

FIGURE 4 — WARNING PERIODS FOR 49 CASES OF FALLS OF 4 mb OR MORE IN 3 hours

T_4 = actual time of start of fall from barograph records;
T_a = time of latest hourly chart used in kinematic method + $1\frac{1}{2}$ hours;
T_b = time of latest hourly chart used in chart-to-chart method + $1\frac{1}{2}$ hours;
T_c = time of issue of warning by forecaster. All times to the nearest $\frac{1}{4}$ hour.
Hatching indicates that warnings were issued after start of fall.

Thus the kinematic method has the advantage of giving ¾ hour extra warning; this is because one more hourly chart normally has to be used to find the isallobaric speed by the 'chart-to-chart' method.

Figures 5 *(a)* and *(b)* show the distribution of the time differences between the actual time of onset (T_4) of the pressure fall and the forecast times of onset, 'T_1' and 'T_2' by the kinematic and chart-to-chart methods respectively. The histograms are not centred around zero since a late forecast was considered to be in more serious error than an early one. The average values of '$T_4 - T_1$' and '$T_4 - T_2$' are both 1 hour 15 minutes, showing that both methods have the same accuracy. Farr (private communication) has shown that the only difference between the calculated speeds of the isallobar by the two methods would be due to the use of finite differences instead of instantaneous derivatives in the kinematic method. The error introduced for this reason is however very small and it was thus expected that the accuracies of the methods would be similar.

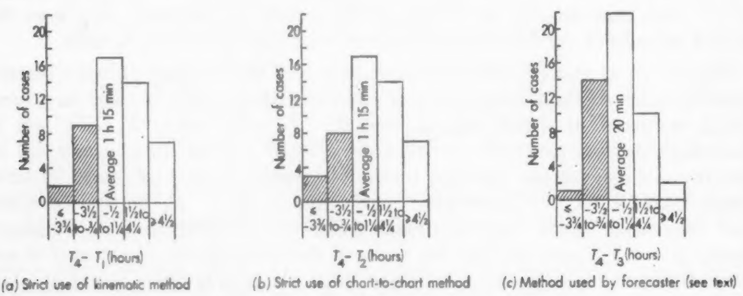

FIGURE 5 — ACCURACY OF FORECAST ONSET TIMES OF FALLS OF 4 mb OR MORE IN 3 hours FOR 49 CASES

T_4 = actual time of start of fall from barograph records;
T_1 = forecast time of start of fall using kinematic methods;
T_2 = forecast time of start of fall using chart-to-chart method;
T_3 = forecast time of start of fall issued by forecaster.
Hatching indicates that fall commenced appreciably earlier than forecast.

Forecasts were also made on a routine basis, prior to the occurrence of the falls, during the six-month period. The forecasters were free to choose, during this period, which method to use and also free to modify the kinematic method if it became obvious that the modifications were resulting in better forecasts. Figure 4 *(c)* shows the distribution of the time difference '$T_4 - T_c$' between the actual onset of the fall and the time 'T_c' of issue of the warning by the forecaster. It was found from experience that if the kinematic method was applied to find the speed of the − 3-mb isallobar when it first appeared on the hourly chart, and this speed was applied to the − 4-mb isallobar if this appeared on the following chart then the warning could be issued a little earlier. Alternatively some forecasters achieved the same benefit by applying the kinematic method to 'adjusted' − 4-mb and − 3-mb isallobars, which were constructed on two successive hourly charts by multiplying by 3 the pressure falls over the hour previous to chart time. This method was used if falls of 3 mb or more in 3 hours were already occurring in the west, and the 'adjusted' − 4-mb isallobar is in fact the locus of points where falls of 4/3 mb have occurred

in the last hour. Warnings of pressure falls were given before the − 4-mb isallobar appeared on the hourly chart; although this resulted in a few cases where warnings were given when falls of 4/3 mb or more in one hour were not maintained and 3-hourly falls were slightly less than 4 mb, these cases were easily outweighed by those where this method produced a greater warning period. Forecasters, over the six-month period, found it beneficial to use the kinematic method, or its modifications as described above, in all cases of pressure falls except those preceding a post-frontal trough where the 'chart-to-chart' method gave better results. Figure 5 *(c)* shows the distribution of time difference '$T_4 - T_3$' between the actual onset of the fall and the forecast time 'T_3' of onset, as issued by the forecaster prior to the event. The improved average time difference of 20 minutes is a result of the two modifications of the 'kinematic' method and of the ability to select between the two basic methods. It should be noted however that the improvement is made marginal owing to the increase in the number of cases where the forecast time of onset was after the actual time.

Longer-period forecasts. The forecasting methods discussed so far are dependent on pressure falls of 4 mb in 3 hours already occurring somewhere in the United Kingdom, and as a result of this the average warning which can be given of this fall occurring in eastern England is about 3½ hours. The 24-hour surface forecast charts issued by Central Forecasting Office, Bracknell, were examined (using data over a period of a year) to see if they could be utilized to give earlier warning. The results showed that it would be inadvisable, at least at present, to forecast pressure falls of 4 mb or more in 3 hours by using 24-hour forecast charts of surface pressure. On such charts errors of timing are introduced and pressure gradients are not always forecast correctly although the 24-hour forecast chart may alert the forecaster to the possibility of large falls during a 24-hour period.

Conclusion. A method of forecasting large pressure falls has been described which is based on the deduction, from a kinematic equation, of the speed of an isallobar appearing on an actual chart. This method is as accurate as the 'chart-to-chart' method and allows the warning of the onset of the pressure fall to be issued earlier. Slight improvement of the kinematic method can be achieved by either of the small modifications suggested on page 316 to give earlier warning. When large pressure falls precede a post-frontal trough the 'chart-to-chart' method gives greater accuracy than the kinematic method of forecasting the time of onset of the large fall. The use of 24-hour forecast charts to forecast pressure falls of this magnitude is, at the moment, inadvisable. It has been found that a considerable improvement in forecasts of pressure falls of 4 mb or more in 3 hours has been achieved, on station, by the formulation and use of the rules described in this paper.

Acknowledgements. The authors are indebted to the staff at Bawtry for carrying out the tests described.

REFERENCES

1. DURST, C. S.; Barometric changes and the efflux of gas in mines. *Prof. Notes met. Off., London*, No. 117, 1956.
2. PETTERSSEN, S.; Weather analysis and forecasting. Vol. I, Second edn,. New York, McGraw-Hill, 1956, p. 45.
3. ECKEL, O.; Mittlere dreistundige Luftdruckänderungen zu den Tagesterminen des internationalen Wetterdienstes. *Annln Hydrogr, Berlin*, **65**, 1937, Heft IV.

551.506.7(548.82):551.507.362.1

METEOROLOGICAL ROCKET SOUNDINGS FROM GAN

By R. J. SHEARMAN

Summary. An account is given, together with an examination of the results, of the first SKUA meteorological rocket sounding campaign from the Island of Gan in the Indian Ocean.

On 25 September 1968 the first SKUA meteorological rocket was launched from the Island of Gan (0°41′S 73°9′E) in the Indian Ocean. Upper air observations are very sparse in equatorial regions, and until this time no soundings had been made above balloon levels within approximately 700 km of the equator. There had been regular launchings from Ascension Island (8°S 14°W) and Fort Sherman (9°N 80°W) and some soundings from Natal, Brazil (6°S 35°W), Thumba, India (9°N 77°E) and Kwajalein, Marshall Islands (9°N 168°W).

Soundings as close to the equator as Gan are particularly interesting because the continuous temperature gradient from the 'winter' to the 'summer' pole at these high levels suggests a cross-equatorial heat flow. The form of this flow will be influenced by the lack of Coriolis force at the equator. Rocket soundings will show how the atmosphere deals with the need for a general N–S flow in conditions of zero Coriolis force.

The quasi-biennial oscillation (the 26-month cycle) is at its strongest below 30 km in low latitudes. It is of interest to see how far it extends above this level, and also to investigate the annual and six-monthly cycles which have appeared in Ascension Island rocket results (Reed[1]).

During the first campaign seven successful launchings were made between 25 September and 10 October 1968. The rockets and sondes used were those described by Almond.[2] Close contact was maintained, on each occasion, with an RAF Shackleton search aircraft until shortly before the instant of firing. The line of fire was on one of three bearings, as directed by this aircraft. This precaution was designed to protect the small native fishing boats which sometimes operate in the area. In fact the launcher bearing was only changed once, and then to avoid a much larger vessel. All but one of the soundings were made after the sun had set at 70 km, so that the sonde was in darkness for the whole of its descent, making radiation corrections unnecessary. Only the last firing took place at local midday, which is the standard launching time throughout the American Meteorological Rocket Network. The conventional radiosonde ground equipment was used to track the sondes and receive their signals.

Apogees of rockets ranged between 57 km and 64 km, somewhat lower (by approximately 5 km) than those attained during regular South Uist firings. This was due to higher densities aloft, and therefore greater drag experienced during the free-flight phase above 16 km. This was partially offset by the ability to fire always at maximum elevation, in consequence of fairly light surface winds.

In the SKUA system the sonde and parachute are ejected just after apogee, about 137 seconds after launch. The rocket body then falls away to splash down at about + 250 seconds. The sonde falls rapidly at first, and the parachute is not considered to be a good wind sensor until it is 4 or 5 km below apogee. Temperatures are recorded from about 3 km below apogee.

Winds. The zonal wind during the sounding period tended to be layered, with light westerlies at the surface, a pronounced band of easterlies from approximately 5 km to 26 km, and another weaker band of easterlies from 37 to 48 km. The heights of the upper and lower boundaries of these layers varied by only 2 or 3 km during the campaign.

The COSPAR* International Reference Atmosphere 1965 (CIRA 1965) includes tables giving mean zonal winds at various heights for each month of the year and for every 10 degrees of latitude and gives estimates of the variability of the wind.

Table I shows the mean zonal wind and extreme values at 2-km intervals, calculated from the Gan soundings, together with CIRA 1965 values for 1 October at 0° latitude. Westerly winds are shown positive.

From 38 km to 48 km there is fairly close agreement between the mean zonal wind and CIRA values. Elsewhere the observed values are within two standard deviations of the values given by CIRA 1965.

The meridional winds were generally light, although northerly components of 17 m/s and 22 m/s were observed at 44 km and, on separate occasions, southerly components of 12 m/s at 40 km and 17 m/s at 52 km.

Diurnal variation of meridional component. All the soundings were made at approximately 1900 local time, except the last which was at 1200. Table II shows the mean meridional component for the evening launches, the extreme values, and the components for the one daylight observation. (Southerly wind is positive).

Groves's[3] value of diurnal variation for stations at around 30°N is about 10 m/s. Several soundings at South Uist (57°N) in June showed a variation of about 12 m/s at 50 km. The maximum change seems to be at approximately 50 km, both from Groves's and from South Uist results.

Below 50 km in Gan, the variability is too great for any estimate to be made of diurnal variation. Above 50 km components at 1200 can be explained in terms of some long-period 'synoptic-type' change, producing a 'trend' in the winds, the trend making the winds more northerly in this case. But between 1900 on 9 October and 1200 on 10 October the diurnal effect is opposed to this trend, making the meridional component more southerly towards midday. Therefore the trend is required to suppress a diurnal change of approximately 10 m/s and still produce a net 'northerly' increase of 5 to 10 m/s. (The trend was of this size above 50 km.) A change of 15 to 20 m/s is required in approximately 17 hours; this is far from impossible, but it is more than double the trend between previous evening soundings. It is possible that the diurnal variation is very much smaller at the equator. However a measurement of the diurnal variation can only be made by soundings which are made at least every six hours and in a series so that long-period type changes can be recognized.

The mean meridional wind was predominantly 'southerly' from 22 km to 40 km, northerly from 40 km to 50 km, southerly from 50 km to 54 km and northerly again above 54 km.

---

* Committee on Space Research of the International Council of Scientific Unions.

TABLE I — ZONAL WINDS FOR GAN, 27 SEPTEMBER TO 9 OCTOBER 1968, AND CIRA 1965 VALUES FOR 1 OCTOBER

Height	Gan zonal wind* Mean	Gan zonal wind* Extremes		CIRA zonal wind*	CIRA standard deviation
km		metres per second			
56	+32	+40	+25	+4	18
54	+34	+41	+31	+4	17
52	+31	+39	+26	+4	16
50	+19	+23	+14	+4	15
48	+5	+13	-6	+4	14
46	+1	+12	-10	+5	14
44	0	+6	-8	+4	13
42	-7	+1	-10	+2	12
40	-10	+6	-19	+1	12
38	-1	+6	-4	-1	11
36	+4	+5	+1	-4	11
34	+9	+12	+4	-7	10
32	+11	+18	+6	-11	9
30	+14	+21	+11	-15	9
28	+12	+15	+8	—	—
26	+1	+7	-8	—	—
24	-31	-24	-41	—	—
22	-27	-23	-33	—	—

* Note : Westerly winds are positive

TABLE II — MERIDIONAL WINDS FOR EVENING SOUNDINGS AND ONE DAYLIGHT SOUNDING AT GAN, 27 SEPTEMBER TO 10 OCTOBER 1968

Height	Gan meridional wind* at approx. 1900 local time Mean	Extremes		Gan meridional wind* at 1200 local time One sounding only
km		metres per second		
56	-4	+4	-20	-26
54	+3	+10	-8	-14
52	+5	+15	-2	-7
50	0	+19	-12	-2
48	-3	+4	-9	0
46	-1	+9	-17	-6
44	-4	+7	-20	-10
42	-5	+7	-17	+6
40	-1	+13	-12	+17
38	+1	+5	-3	+5
36	+1	+4	-1	0
34	-3	+2	-9	-2
32	+1	+5	-6	-3
30	+1	+9	-2	-3
28	-2	+3	-7	+1
26	0	+5	-5	-4
24	+4	+6	-1	+9
22	+3	+5	-2	-2

* Note: Southerly winds are positive

Temperature. Figure 1 shows the range of observed temperatures for the sunset soundings, during the Gan campaign, at kilometre intervals, together with the corresponding CIRA 1965 profile and lower limit of variability. This variability was originally calculated by taking the difference between observed temperatures and the model, and because of lack of observations it can be expected to be exceeded on 50 per cent of occasions (Groves[4]). Accepting this, the agreement between the two profiles is remarkably good, particularly as CIRA 1965 was not adjusted for diurnal effects, and was constructed from American rocket temperatures, which were measured at local midday, whereas the first six Gan soundings were all made at 1900 local time in darkness.

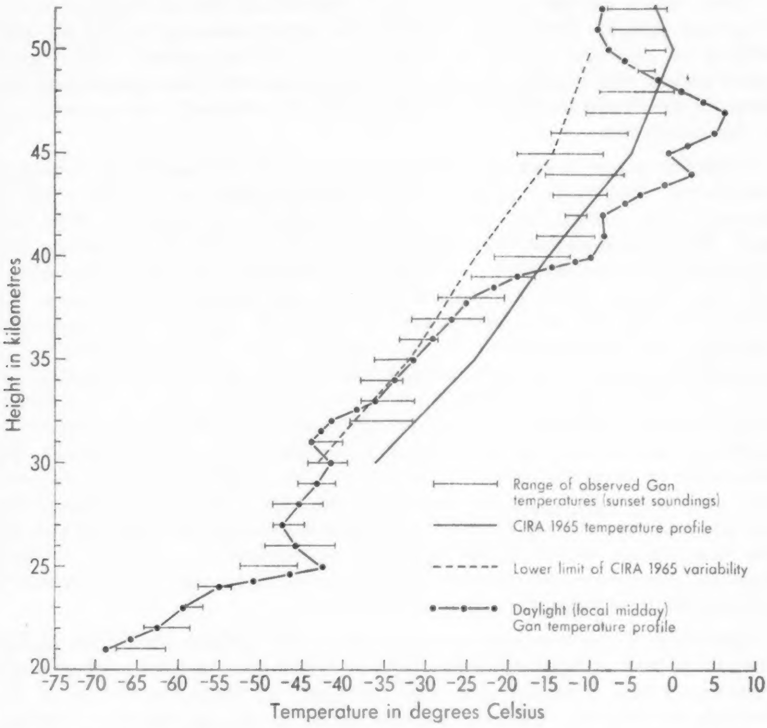

FIGURE 1 — COMPARISON OF OBSERVED TEMPERATURE AT GAN FOR LATE SEPTEMBER AND EARLY OCTOBER 1968 WITH COSPAR INTERNATIONAL REFERENCE ATMOSPHERE 1965

The one daylight temperature sounding from Gan indicated temperatures approximately 5 degC higher than those from the sunset firings, between 44 and 47 km (Figure 1). Table III shows the sequence of temperatures measured at the appropriate heights.

TABLE III — SEQUENCE OF TEMPERATURES AT GAN FROM 27 SEPTEMBER TO 10 OCTOBER 1968

Height	September			October			
	27	28	30	4	7	9	10*
km				*degrees Celsius*			
47	−8·7	−0·8	−3·7	−6·9	−3·0	−8·9	+3·9
46	−13·0	−6·8	−4·6	−4·8	−8·6	−9·8	+5·6
45	−17·3	−8·5	−7·4	−7·7	−8·2	−9·7	+1·9
44	−16·9	−14·3	−10·7	−8·5	−10·9	−6·0	+1·3
Mean 44–47	−14·0	−7·6	−6·6	−7·0	−7·7	−8·6	+3·2

* Daylight sounding

There was a change of about 6 degC between 27 and 28 September, i.e. a 24-hour period. The change between the sunset sounding on the 9th and midday on the 10th is about 12 degC, over a 17-hour period. This seemed rather violent, and computational errors were suspected; subsequent checking, however, has shown nothing abnormal in either the original temperature traces or the calculations.

A possible source of error is radiation heating of the resistance-wire temperature sensor. The correction given by laboratory experiments for this height is approximately 4 degC, i.e. the temperature given by the sensor is 4 degC too high. In addition to this direct solar heating, there is reflected radiation, and long-wave radiation from the surrounding atmosphere. The reflected component was taken to be 10 per cent of the normally incident radiation, as the sonde was over the sea, and cloud was relatively sparse. The long-wave radiation was neglected both by day and by night, and is thought to be negligible compared with reflected solar radiation by day. At the equinox, in Gan, the sun is directly overhead at 1200 local time, so the temperature element swings regularly into and out of the shade of the parachute and its sonde. At the extremes of the swing it is completely exposed to the sun, the semi-angle of swing being greater than 45°. (Australian workers have used two cameras at right-angles in place of a sonde, and from the gyrations of the horizon and the frame speed have calculated the period and angle of swing.) The temperature record of this flight shows a regular temperature variation of 4 degC every 6 seconds, the normal period of swing for this parachute, which indicates that the laboratory correction is realistic.

Theoretically the temperatures at 1900 at these heights should be higher than, or at least comparable with, those at 1200,[4] since the cosine law which holds for heating a surface area does not apply in heating a volume of the atmosphere. Heating will only decrease owing to passage through a thicker layer of atmosphere later in the day, and will therefore fall off more slowly than at the surface. There is also a lag between maximum heating rate and the attainment of maximum temperature.

If the radiation corrections are reasonably accurate, the theoretical diurnal effect holds, and computational errors are ruled out, then there seems to have been a strong synoptic-scale change between sunset on 9 October and midday on 10 October.

Variation in pressure surfaces. In the stratosphere in mid-latitudes there are large pressure changes attributable to travelling disturbances. Since there is a strong temperature gradient between 'summer' and 'winter' hemispheres in the stratosphere, a cross-equatorial heat transfer can be expected. This is likely to be most efficiently performed by such travelling synoptic-scale disturbances, in addition to the meridional circulation described by Murgatroyd and Singleton.[5] The Gan soundings were therefore studied for evidence of these systems.

Figure 2 shows the heights of the 10-mb, 5-mb and 1-mb surfaces from 27 September to 9 October 1968. These observations seem to indicate the passage of a synoptic-scale disturbance, which was at its strongest at the 1-mb level, with a change in contour height of more than 350 m. Changes of 250 m and 200 m occurred at the 5-mb and 10-mb levels respectively. The magnitude

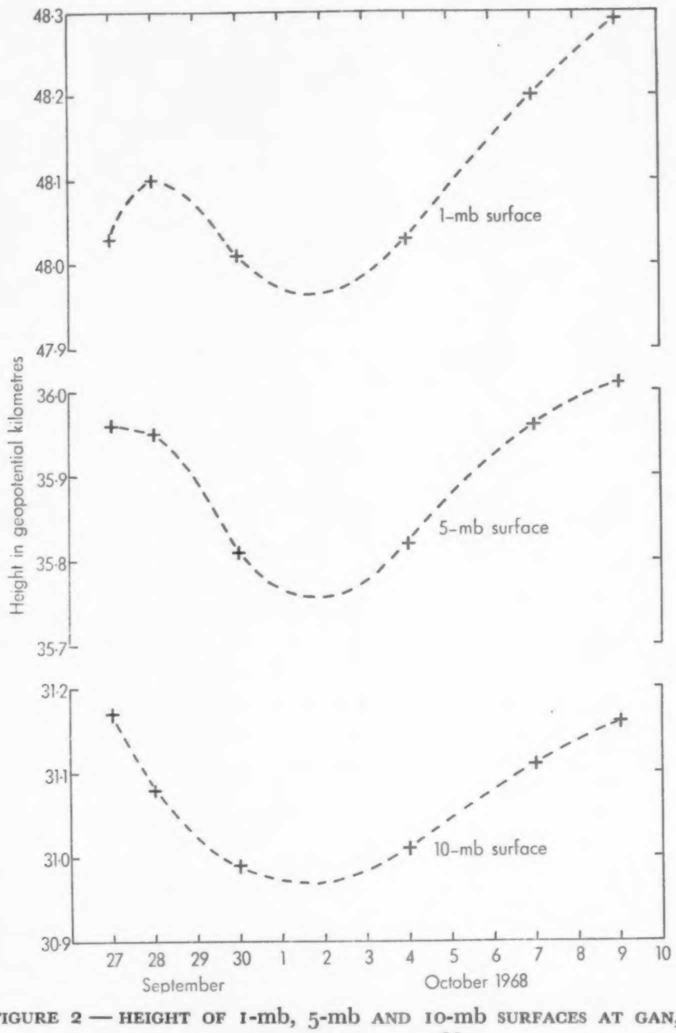

FIGURE 2 — HEIGHT OF 1-mb, 5-mb AND 10-mb SURFACES AT GAN, SEPTEMBER–OCTOBER 1968

of the disturbance fell off with decreasing height, being barely detectable at 100 mb ($\approx$ 16 km). Figure 3 shows a similar disturbance of the zonal wind component at Ascension Island at 50 km ($\approx$ 0·8 mb) and 40 km ($\approx$ 3 mb) in both 1965 and 1966, on nearly the same time scale as the Gan system.

Future campaigns in Gan. It is intended to make a series of launchings each year from Gan. An agreement has been drawn up between the British and Indian governments, enabling the United Nations range at Thumba

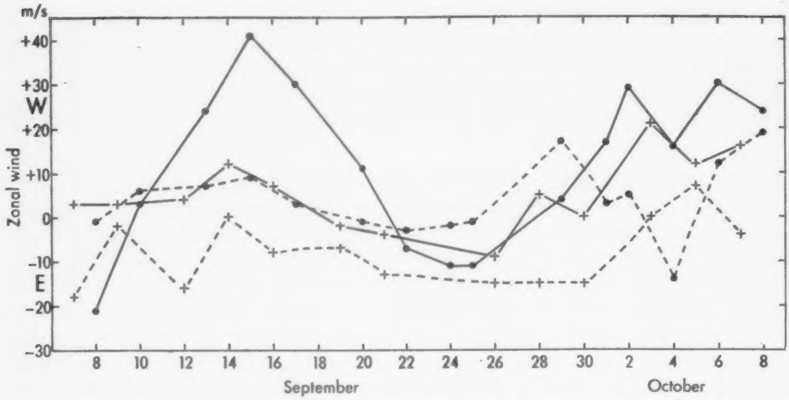

FIGURE 3 — ZONAL WIND AT ASCENSION ISLAND, SEPTEMBER–OCTOBER 1965 AND 1966

————	Zonal wind at 50 km 1965	+———+	Zonal wind at 50 km 1966
- - - - -	Zonal wind at 40 km 1965	+ - - - +	Zonal wind at 40 km 1966

Westerly winds are positive

(8°32′N 76°57′E) to launch a number of SKUA rockets with standard Meteorological Office rocket-sonde payloads. It is hoped to carry out this programme in conjunction with a three-week campaign in Gan.

Acknowledgements. On behalf of the SKUA meteorological rocket team I would like to express appreciation for the co-operation and assistance of the personnel of Royal Air Force, Gan. Our thanks are also due to the radiosonde staff, who were extremely helpful at all times.

REFERENCES

1. REED, R. J.; The present status of the 26-month oscillation. *Bull. Am. met. Soc., Lancaster, Pa*, **46**, 1961, p. 374.
2. ALMOND, R.; Techniques of temperature and wind sounding with the SKUA meteorological rocket. *Met. Mag., London*, **94**, 1965, p. 327.
3. GROVES, G. V.; Diurnal and semi-diurnal S–N wind components in the upper atmosphere derived from rocket measurements. R. L. Smith-Rose (editor); Space Research VI, Volume II. Amsterdam, North-Holland Publishing Company, 1967, p. 986.
4. GROVES, G. V.; Comparison of new results with the CIRA 1965 with emphasis on the IQSY data. A review for the region 30 to 100 km. R. L. Smith-Rose (editor); Space Research VIII. Amsterdam, North-Holland Publishing Company, 1968, p. 23.
5. MURGATROYD, R. J. and SINGLETON, F.; Possible meridional circulations in the stratosphere and mesosphere. *Q.Jnl.R. met. Soc., London*, **87**, 1961, p. 125.

OBITUARIES

It is with regret that we have to record the death of Mr H. J. Matthews, Senior Scientific Assistant, on 3 August 1969, and of Mr C. P. Brohan, Scientific Assistant, on 21 August 1969.

THE METEOROLOGICAL MAGAZINE

VOL. 98 NO. 1167 OCTOBER 1969

CONTENTS

NOTICES

It is requested that all books for review and communications for the Editor be addressed to the Director-General, Meteorological Office, London Road, Bracknell, Berkshire, RG12 2SZ, and marked 'for Meteorological Magazine.'

The responsibility for facts and opinions expressed in the signed articles and letters published in this magazine rests with their respective authors.

All inquiries relating to the insertion of advertisements in the Meteorological Magazine should be addressed to the Director of Publications, H.M. Stationery Office, Atlantic House, Holborn Viaduct, London E.C.1. (Telephone: CITy 9876, extn 6098).

The Government accepts no responsibility for any of the statements in the advertisements appearing in this publication, and the inclusion of any particular advertisement is no guarantee that the goods advertised therein have received official approval.

Printed in England by The Bourne Press, Bournemouth, Hants.

and published by

HER MAJESTY'S STATIONERY OFFICE

3*s*. 6*d*. monthly **Annual subscription £2 7*s*. including postage**

Dd. 152073 K16 10/69 SBN 11 400067 0